

Research Article

Ivica Milevski*, Bojana Aleksova, Tin Lukić, Slavoljub Dragičević, and Aleksandar Valjarević

Multi-hazard modeling of erosion and landslide susceptibility at the national scale in the example of North Macedonia

<https://doi.org/10.1515/geo-2022-0718>

received May 31, 2024; accepted September 25, 2024

Abstract: Due to favorable natural conditions and human impact, the territory of North Macedonia is very susceptible to natural hazards. Steep hillslopes combined with soft rocks (schists on the mountains; sands and sandstones in depressions), erodible soils, semiarid continental climate, and sparse vegetation cover give a high potential for soil erosion and landslides. For this reason, this study presents a multi-hazard approach to geohazard modeling on the national extent in the example of North Macedonia. Utilizing Geographic Information Systems, relevant data about the entire research area were employed to analyze and assess soil erosion and susceptibility to landslides and identify areas prone to both hazards. Using the Gavrilović Erosion Potential Method (EPM), an average value of 0.36 was obtained for the erosion coefficient Z , indicating low to moderate susceptibility to erosion. However, a significant area of the country (9.6%) is susceptible to high and excess erosion rates. For the landslide susceptibility assessment (LSA), the Analytical hierarchy process approach is combined with the statistical method (frequency ratio), showing

that 29.3% of the territory belongs to the zone of high and very high landslide susceptibility. Then, the accuracy assessment is performed for both procedures (EPM and LSA), showing acceptable reliability. By overlapping both models, a multi-hazard map is prepared, indicating that 22.3% of North Macedonia territory is highly susceptible to erosion and landslides. The primary objective of multi-hazard modeling is to identify and delineate hazardous areas, thereby aiding in activities to reduce the hazards and mitigate future damage. This becomes particularly significant when considering the impact of climate change, which is associated with increased landslide and erosion susceptibility. The approach based on a national level presented in this work can provide valuable information for regional planning and decision-making processes.

Keywords: natural hazards, geohazards, hazards assessment, excess erosion, landslides, GIS, remote sensing

1 Introduction

Natural processes and human activities shape the environment and can lead to natural hazards, including prominent geohazards [1]. Although they may not always pose the greatest threat to humanity, their impacts can vary significantly, influenced by different levels of vulnerability. This variability underscores the importance of employing multi-hazard techniques for comprehensively analyzing hazardous events. According to Aleksova et al. [2], the multi-hazard approach involves identifying and evaluating the major hazards that a region faces, considering the potential for these hazards to occur simultaneously, cascade, or accumulate over time, and understanding their interrelated effects. The multi-hazard approach is crucial because it unifies susceptibility, vulnerability, and hazard assessment within a single framework. This method allows for a comprehensive evaluation, essential for spatial planning, by identifying hazard-prone areas, assessing vulnerabilities of natural and human-made elements, and categorizing hazard zones based on varying

* **Corresponding author: Ivica Milevski**, Institute of Geography, Faculty of Natural Sciences and Mathematics, Ss. Cyril and Methodius University, Gazi Baba, Arhimedova 1000, Skopje, North Macedonia, e-mail: ivica@pmf.ukim.mk

Bojana Aleksova: Department of Geography, Tourism and Hotel Management, Faculty of Sciences, University of Novi Sad, Trg Dositeja Obradovića 3, 21000, Novi Sad, Serbia; Scientific-Professional Society for Disaster Risk Management, Dimitrija Tucovića 121, 11040, Belgrade, Serbia; International Institute for Disaster Research, Dimitrija Tucovića 121, 11040, Belgrade, Serbia

Tin Lukić: Department of Geography, Tourism and Hotel Management, Faculty of Sciences, University of Novi Sad, Trg Dositeja Obradovića 3, 21000, Novi Sad, Serbia; Scientific-Professional Society for Disaster Risk Management, Dimitrija Tucovića 121, 11040, Belgrade, Serbia; International Institute for Disaster Research, Dimitrija Tucovića 121, 11040, Belgrade, Serbia

Slavoljub Dragičević, Aleksandar Valjarević: Faculty of Geography, University of Belgrade, Studentski Trg 3/III, 11000, Belgrade, Serbia

levels of risk. Developing a multi-hazard map is a critical first step in preventing and mitigating natural hazards, enabling the systematic analysis of multiple hazards both independently and in combination [3–9].

As a result of suitable natural factors and high human impact over centuries, North Macedonia is highly susceptible to a range of natural hazards and prominent geohazards like severe erosion, landslides, rockfalls, and torrential floods [10–16]. Characterized by erodible crystalline rocks, sandstones, lacustrine and fluvial deposits, steep slopes (39.5% exceeding 15°), a semiarid climate (annual precipitation 500–600 mm), and sparse vegetation, North Macedonia experiences significant soil erosion (Figure 1). This erosion is primarily a result of historical deforestation and improper land use, leading to severe consequences including landscape degradation and substantial economic damage [10,14]. In Europe, soil erosion vulnerability is assessed using qualitative, quantitative, and model-based methods [17–19]. Although well-known empirical models such as USLE [20], PESERA [21], KINEROS [22], WEP [23], and WEPP [24,25] are widely used, locally adapted models like the Erosion Potential Model (EPM) [18,26] also demonstrate proven accuracy. Over the past two decades, the development of geospatial databases using Geographic Information Systems (GIS) technology has improved these models, including EPM [27,28].

Landslides present another major threat in North Macedonia, frequently triggered by intense rainfall or

rapid snowmelt (Figure 2). Construction activities, particularly in vulnerable terrains, exacerbate landslide occurrences [29]. Accurate identification and mapping of landslide-prone areas are crucial, often achieved through Landslide susceptibility zonation (LSZ) techniques [30]. GIS and remote sensing tools are essential for evaluating landslide-prone areas by integrating spatial data to assess the impact of causative factors. Landslide susceptibility methods are categorized into qualitative (heuristic) and quantitative, with hybrid approaches often used when datasets are insufficient for robust statistical analysis [30–33].

The United Nations Office for Disaster Risk Reduction (UNDRR) emphasizes the multi-hazard concept, which involves identifying multiple hazards a region may face and the conditions under which these hazards may occur simultaneously, sequentially, or cumulatively while considering potential interconnected effects [2]. Effective hazard analysis relies on applying multi-hazard techniques [2–9,11,17], and integrating probabilistic and deterministic stochastic processes offers an alternative approach [6].

Incorporating resilience – the ability of a system to absorb and recover from hazardous events – is also crucial in this context. Resilience encompasses the capacity to withstand and recover from impacts, the adaptability to changing conditions, and the ability to reduce vulnerability over time.

Given these considerations, it is imperative to develop models at a national scale for assessing potential erosion and



Figure 1: Notable sites in North Macedonia with excess erosion: (a) Kratovska River valley; (b) Ribnica valley; (c) Ski-slopes on Kožuf Mt.; and (d) Kamenica River valley.



Figure 2: Some of the remarkable landslides in North Macedonia: (a) Landslides along the highway Petrovec-Štip; (b) Stanci landslide near Kriva Palanka; (c) Sasa landslide in Kamenica River valley; and (d) Kosevica landslide.

landslide susceptibility in North Macedonia. This research represents the first attempt to create a multi-hazard map combining both types of hazards. The primary objectives are: (1) assessing erosion and landslide susceptibility using modified models; (2) generating multi-hazard susceptibility maps; and (3) identifying areas with the highest vulnerability to inform the development of effective mitigation measures [10–16]. This study addresses soil erosion and landslide vulnerability through a comprehensive GIS-based approach, integrating well-established empirical and successful local models. Enhancing land use practices and forest rehabilitation are critical for managing these hazards. This approach supports spatial planning and disaster management decision-making by providing efficient, cost-effective, and wide-area hazard zone identification [33].

2 Data and methodology

2.1 Study area

North Macedonia, encompassing an area of 25,713 km² in the southern Balkan Peninsula, is predominantly mountainous (79%), while plains cover just 19%, and the rest 2% are lakes and reservoirs (Figure 3). The landscape features frequently changes in mountains and valleys, resulting in

a high average slope of 15.4°, with 39.5% of the territory having slopes steeper than 15° [34]. Geologically, the territory of North Macedonia belongs to six geotectonic units, exhibiting diverse lithology ranging from Precambrian to Cenozoic rocks [35]. The prevalence of highly erodible crystalline and clastic sedimentary rocks, especially at foothills, makes these areas susceptible to erosion and landslides. As a result of the chequerboard topography, the climate is variably influenced by Mediterranean, continental, and mountainous factors. Due to climate change, this semiarid area with annual precipitation of about 500–700 mm has suffered more frequent storms and heavy rain events in recent decades, contributing even further to erosion and landslide occurrences [36]. Sudden winter-to-spring penetrations of hot Mediterranean air frequently lead to rapid snowmelt and high overland flow, activating large landslides and avalanches [37].

Human activities, urbanization, and infrastructure expansion into hazard-prone areas exacerbate the impact of natural factors [38].

2.2 Methodology for soil erosion assessment

For the assessment of soil erosion intensity, the EPM, also known as the Gavrilović method [26], is widely used in the



Figure 3: Geographical location of North Macedonia.

Balkans and beyond, including Serbia, Croatia, Slovenia, Germany, Italy, Argentina, Belgium, North Macedonia, Greece, etc. [18,39–44]. It reliably assesses soil erosion rate, estimates mean annual soil loss and sediment yield, and helps plan erosion control works and torrent regulation on a regional scale. The method relies on the following equation:

$$Wy = T \cdot H \cdot \pi \cdot \sqrt{Z^3} \cdot f,$$

where Wy represents the average annual erosion rate in m^3 ; T is the temperature coefficient, calculated as $T = (0.1 \cdot t + 0.1)^{0.5}$, with t being the mean annual air temperature; H indicates the mean annual precipitation in mm; Z is the erosion coefficient, ranging from 0.1 to 1.5 and more; and f is the studied area in km^2 . Among these factors, the coefficient Z has the highest importance, as it combines rock and soil erodibility (Y), land cover index (Xa), index of visible erosion processes (ϕ), and mean slope of the catchment (J) in the ratio

$$Z = Y \cdot Xa \cdot (\phi + \sqrt{J}).$$

Originally, the EPM method was heuristic, generally based on expert estimations of the parameters on the field. Because of that subjectivity, GIS-based approaches have been developed and updated recently, and they heavily rely on deriving most parameters from digital elevation models, thematic maps, and satellite images [11,14,27,28,45].

Thus, in our study, 15 m digital elevation model (DEM) from the Ministry of Agriculture, Forestry, and Waters is used (originally 5 m DEM corrected and interpolated to 15 m DEM). For the Y coefficient, a previously digitized geological (100 k) [46] and soil map (50 k) [47] were rasterized to 15 m to correspond to the used DEM resolution, and erodibility values were added according to Gavrilović's approach [26]. These values generally range from 0.1 for resistant rocks to 2.0 for non-resistant rocks and soils (Table 1).

However, accurately quantifying coefficient Y poses challenges because of the field's different soil and rock combinations and compactness. Thus, a fitting procedure with rooting is used in the form $Y = \sqrt{Y1}$. The land cover index, Xa , is derived from the CORINE Land Cover (CLC) model (CLC2018) [48], with values ranging from 0.1 (indicating dense forests) to 1.0 (indicating bare rocks) based on Gavrilović [26] values (Table 2).

The values for the coefficient ϕ (visible erosion processes) are determined from the Bare Soil Index (BSI), which is based on Landsat 8 or Sentinel 2 imagery [45]. The Sentinel 2-based BSI used in our study (BSI S2) is calculated from the values of the spectral bands B, according to the form:

$$BSI\ S2 = ((B11 + B04) - (B08 + B02)) / ((B11 + B04) + (B08 + B02)).$$

Table 1: Some values of the soil and rock erodibility (γ)

Type	Value
Regosol	1.20
Podzols, schists	1.00
Dystic Cambisol	0.80
Vertisol, fluvisol, luvisol	0.60
Tuffs	1.60
Ranker	0.90
Alluvial deposits	0.50
Clastic sediments	2.00
Compact limestone and marble	0.20
Decomposed carbonate rocks	1.20
Compact volcanic rocks	0.20

Table 2: Values of the land cover coefficient (X_a)

Type	Value
Discontinuous urban fabric	0.25
Nonirrigated arable land	0.80
Pastures	0.50
Land principally occupied by agriculture	0.55
Broad-leaved forest	0.20
Coniferous forest	0.15
Mixed forest	0.15
Natural grasslands	0.40
Moors and heathland	0.50
Transitional woodland-shrub	0.40
Sparsely vegetated areas	0.90

In some studies, instead of BSI, the red spectral band of Landsat 7/8/9 or Sentinel 2 scene is used as $\varphi = a/255$, where a is the greyscale pixel value. The results are between 0 and 1, where the lower values indicate areas without visible erosion processes, while higher values show sites with severe erosion processes [11,13–16]. However, further research will show the eventual advantage of each approach.

The average terrain slope (J) was calculated from a 15 m DEM, expressed in decimal percentage [49]. It is recognized that higher slopes correspond to reduced stability, increased erosion potential, and increased susceptibility to torrential floods, as noted by Durlević et al. [50]. With all of the above, the GIS-calibrated coefficient Z is determined by the equation:

$$Z = \sqrt{Y} \times X_a \times (((BSI+0.3) \times \sqrt{J})) + \sqrt{J})).$$

Climate parameters (T and H) are derived from the average air temperature and precipitation models for the period 1991–2020, based on the interpolation of WorldClim v.2 [51], MODIS LST [51,52], and the data from the National Hydrometeorological Service. Multiplied climate potential, Z erosion coefficient, and study area (in km^2) determine the

mean annual soil loss in m^3 (Wy). The GIS-based EPM approach has been tested in various regions in North Macedonia [2,11,13–15] and other countries [44,53–62].

2.3 Methodology for landslide susceptibility assessment (LSA)

The modeling and mapping of landslide-prone areas on a regional scale represent a highly complex task due to the numerous natural and anthropogenic factors associated with landslide processes. Consequently, the LSA results from prior research in the country were incorporated into this study [11–13,15,63]. A crucial step in LSA is having a good landslide inventory. However, North Macedonia lacks a comprehensive inventory despite numerous landslides, favorable natural conditions, and high human impact. For our research, the existing dataset of 302 landslides from the previous national-scale work [12] is updated with an additional 198 landslides (as georeferenced vector points), comprising a total of 500. Various data sources were used to compile the dataset, including maps, scientific papers, media reports, field surveys, and satellite imagery. Most landslides were rotational and translational types, as well as rock falls and earth falls (e.g., [64]). A random split into training (250 landslides) and validation (250 landslides) datasets was performed. The training dataset facilitated statistical analysis for modeling, while the validation dataset was used to verify the model's results [12]. This methodology aligns with established practices in landslide susceptibility research [32]. The next step in the procedure was to identify the primary landslide factors. Topography, lithology, and land use are essential for GIS analysis [63–65], although other factors like tectonic features and rainfall distribution can also be influential [66]. E.g., Milevski et al. [12], for the same area, underscored the evaluation of eight triggering factors from which six are identified as most important, including lithology, slope angle, land cover, terrain curvature, distance from rivers, and distance from roads. These factors are selected in our study (Table 3), and they are the foundation for various LSA methods [67].

The subsequent step involves selecting a suitable LSA method. Considering the large areal extent and the very limited landslide inventory, a combination of the frequency ratio (Fr) and Analytical Hierarchy Process (AHP) methods is employed. The frequency ratio method, recognized as highly effective for larger areas [68], is grounded in the relationship between the spatial distribution of landslides and each conditioning factor [69]. This method calculates the Landslide susceptibility index (LSI) for each

category i of all selected factors j (e.g., slope, lithology, land cover, etc.). The calculation is performed using the following equation proposed by He and Beighley [70]:

$$LSI_{ij} = \ln \left(\frac{N_{ij}}{A_{ij}} / \frac{N_T}{A_T} \right),$$

where N_{ij} represents the number of landslides in category j of factor i , A_{ij} denotes the area of this category, N_T is the total number of landslides, and A_T is the total area under investigation. If a category (or selected factor) strongly correlates with landslides, the associated area will exhibit a notably high positive LSI. Conversely, a negative LSI value for a specific category signifies a low density of landslides in that class [12]. Consequently, LSI presents the relative susceptibility to landslide occurrence. The final LSI is generated by summing up all triggering factors' values for a grid cell of all six digital layers.

The AHP approach is a semi-qualitative method that involves matrix-based pairwise comparisons of different factors' weight contributions to landsliding. A pairwise comparison matrix is compiled using three expert opinions and frequency ratio range and rankings. These weights signify the relative importance of each factor in triggering landslides within the catchment, with slope being the most influential factor, followed by lithology, land cover, planar curvature, and distance to streams and roads [12]. As with the LSI approach, in the AHP approach, the final map is calculated by summing up the values of individual grid cells of all digital layers [63].

The final LSA model is created from the mean LSI + AHP values. Subsequently, by natural breaks classification, the continuous values are classified into five distinct classes: very low, low, medium, high, and very high landslide susceptibility zones. Natural breaks and quantile classification methods are commonly utilized without a widely accepted agreement on the best approach for classifying LS values

[68–75]. However, the natural breaks algorithm [76] is preferred in this study for its effectiveness when the LSI histogram exhibits distinct breaks [77,78].

2.4 Methodology for multi-hazard modeling

Developing a comprehensive multi-hazard model entails the integration of models of potential erosion and landslide susceptibility into a unified framework. Following Aleksova *et al.* [16] work, pertinent GIS tools within QGIS 3.34 and SAGA GIS 9.3.0 software were judiciously employed to delineate multi-hazard areas. First, values from previously produced EPM and landslide susceptibility models are classified into five classes: very low to very high potential or susceptibility. Then, the very high classes of both models are considered and reclassified as class one for erosion and class two for landslides. With a simple addition of both, the multi-hazard class as class three is calculated.

The resulting multi-hazard model, designed to account for the convergence of both geohazards, assesses the likelihood of one or two hazards occurring in a specific area. To enhance the efficacy of this approach, a synthesis of methodologies was employed, combining on-the-ground field analysis with sophisticated statistical techniques facilitated by GIS software. This holistic strategy aims to provide a nuanced understanding of the geohazard landscape, yielding more accurate and actionable results. Following the UNDRR, the multi-hazard concept considers circumstances under which hazardous events may manifest concurrently, progressively, or cumulatively over time, acknowledging potential interconnected effects [79]. The significance of employing multi-hazard techniques in hazard event analysis is underscored in the literature [2–9,11,13,15–17,62,80].

Table 3: Data sources for landslide susceptibility analysis

Data type	Source	Details	Relevance
Lithology	Digitalized geological map (100 k)	Focused on seven distinct lithological units within the municipality area.	Provides lithological composition data for landslide analysis.
Slope and plan curvature	15 m DEM	Derived from a 15 m DEM.	Key for understanding terrain morphology and its influence on landslides.
Land use	CORINE land cover 2018 classification hierarchy	Extracted land cover types within the study area.	Aids in assessing landslide susceptibility based on land cover types.
Distance from streams	Topographic river networks	Distances calculated with buffer zones (20 m increments) and converted to raster format.	Proximity to streams influences landslide susceptibility.
Distance from roads	Open street map road networks	Distances calculated with buffer zones (20 m increments) and converted to raster format.	Proximity to roads influences landslide susceptibility.

3 Results

3.1 EPM

With the suggested EPM approach, the models of erosion coefficient Z and the mean annual erosion rate W were produced, maintaining a resolution of 15 m and aligning with the input layer datasets. The erosion coefficient Z model delineates values ranging from 0, indicative of areas without erosion (or deposition sites), to values exceeding 1.5, representing areas with severe (excessive) erosion (Figure 4). The average Z value for the entire country is 0.36, which corresponds to low-to-moderate erosion. Nevertheless, extensive regions covering 9.6% exhibit high erosion vulnerability, with a Z value above 0.7 (Table 4). In these regions, even modest rainfall triggers substantial production of eroded material. This phenomenon is particularly noticeable during heavy rainfalls exceeding 30 mm/day.

According to the used approach, the average annual erosion rate (W_y) for the territory of North Macedonia is moderate to high, measuring $516.4 \text{ m}^3/\text{km}^2$ or 0.52 mm/year.

Table 4: Areas under different erosion susceptibility classes (according to Z -values of EPM)

Susceptibility	Class	In km^2	In %
Very low	0–0.2	6294.6	24.5
Low	0.2–0.4	10011.8	38.9
Moderate	0.4–0.7	6525.9	25.4
High	0.7–1.0	2130.5	8.3
Very high	>1.0	324.9	1.3
Lakes	—	425.3	1.7
Total		25713.0	100.0

This is significantly less than the findings from the traditional Erosion map ($685.0 \text{ m}^3/\text{km}^2$ according to Djordjević et al. [36]) prepared generally in the 1980s. Thus, to check the accuracy of the implemented EPM approach, a comparison is usually made with the measurement of sediment deposition in reservoirs. Because of the available data, our study compares the average annual sediment deposition from the upper Bregalnica catchment (1124.7 km^2) to Kalimanci Lake (reservoir). Hence, with the EPM approach, the

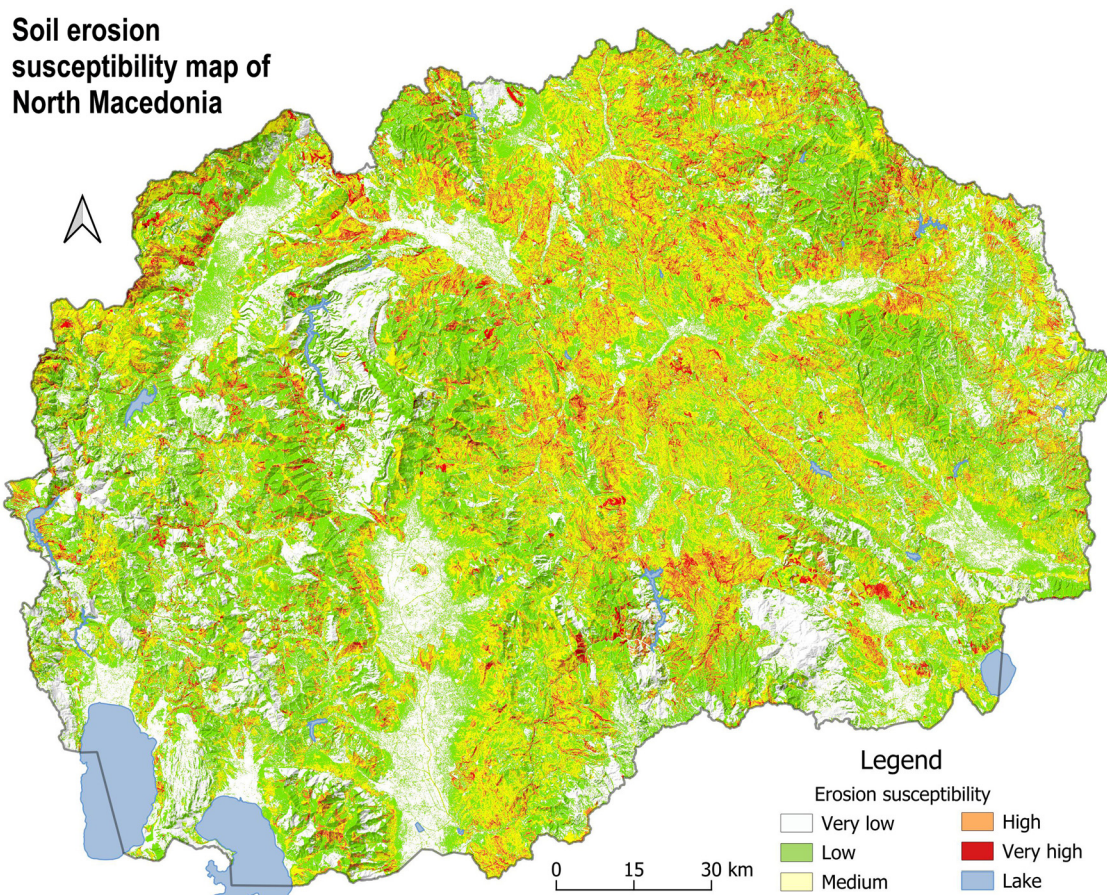


Figure 4: Erosion susceptibility map of North Macedonia (according to Z coefficient values).

sediment delivery ratio (R_u) is estimated using the following equation:

$$R_u = \sqrt{(O \times D)/0.25 \times (L + 10)},$$

where O represents the length of the watershed border in km, D signifies the difference between the average altitude and the altitude of the catchment outlet in km, and L is the catchment length [26]. The sediment yield (G) is then calculated as follows:

$$G = W \times R_u,$$

According to the calculations, the R_u value for the upper Bregalnica catchment is 0.38, and the average annual sediment yield (G) from the catchment to the Kalimanci Lake totals 236,943 m³/year. This value is just 10% higher than the recent echo sonar measurements of sediment deposition in Kalimanci Lake [81], according to which the average annual sediment deposition in Kalimanci Lake is 214,325 m³/year. That shows the high accuracy of our EPM approach, which needs to be further checked with additional measurements on the mentioned rivers. Thus, the difference with the

previous (traditional) erosion map [36] is probably because of the decreased erosion rate due to the substantial depopulation of rural areas in the last decades and the different approaches used in both procedures.

Aside from the mentioned differences, the spatial distribution of erosion classes exhibits some similarities. The erosion rate (W_y) typically ranges between 0 and 500 m³/km²/year in flats or densely forested mountainous regions. Contrary to that, certain rural areas experiencing significant human impact show erosion rates exceeding 1,000 m³/km²/year (Figure 5). The areas with the highest erosion rates (excess erosion) are identified in the catchments of Bregalnica, Crna River, Pčinja, Kriva Reka, Pena, etc., giving rise to destructive landforms, the loss of valuable fertile land, and the substantial filling of riverbeds with sediment.

With further analysis, the annual erosion rate has been segmented into five classes, ranging from very low erosion or deposition to severe (excess) erosion.

The findings in Table 5 emphasize the prevalence of terrains exhibiting low to very low erosion rates,

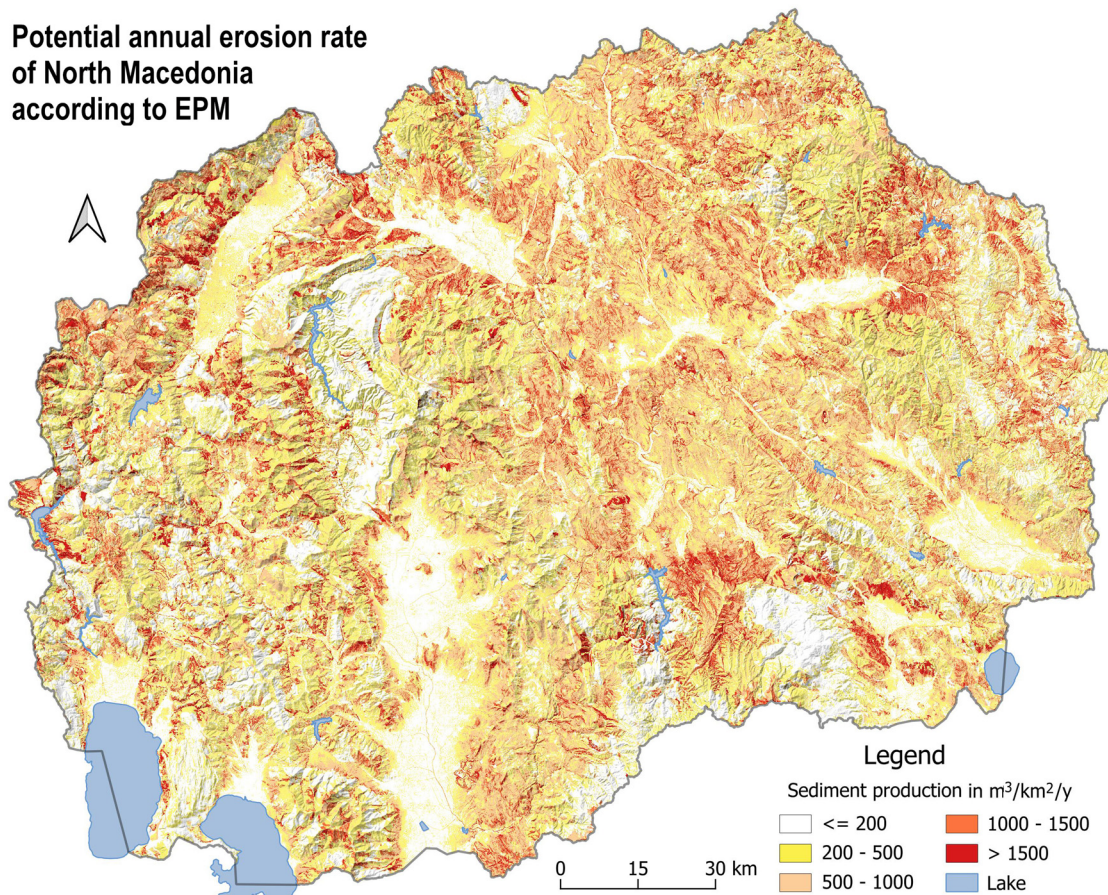


Figure 5: Potential annual erosion rate of North Macedonia.

Table 5: Erosion rate classes in North Macedonia according to EPM

Class	m ³ /km ² /year	In km ²	In %
Very low	0–200	6757.5	26.3
Low	200–500	9056.3	35.2
Moderate	500–1,000	6043.2	23.5
High	1,000–1,500	2401.0	9.3
Very high (severe)	>1,500	1029.7	4.0
Lakes	—	425.3	1.7
Total		25713.0	100.0

constituting 61.5% of the total. These areas are associated with densely forested, gentle-slope mountain regions and plains in depressions. Deposition sites are linked to lakes, reservoirs, and downstream segments of larger rivers, resulting in their comparatively lower mean elevation when compared to other classes. As per the model, substantial proportions of the country encompass regions with high erosion rates, totaling 13.3%. These areas are dominantly located on steep, exposed, and erodible hilly mountain slopes. Such erosion rate often leads to a landscape marked by rills, gullies, badlands, and earth pyramids.

3.1.1 Landslide susceptibility model

As the previous research [12] shows, for the area of North Macedonia, and with a very limited landslide dataset, the mean value of the combined LSI and AHP models produces LSA map with acceptable accuracy; thus, the same approach is used in this study.

The LSI model is based on summing up the values of all six triggering parameters, with subsequent classification into susceptibility zones. The results indicate that the 0–50 m road buffer exhibits the highest positive LSI value. However, this outcome might be influenced by the nature of the landslide dataset, where many landslides and rock-falls occur on roadside slopes. Despite this, the relative significance ratios between classes for each factor align well with expectations from field analysis. Except for the

road factor, the most crucial factors are slope, lithology, and land cover (Table 6). All factors, except convexity (planar curvature), exhibit a values range (between LSI_{min} and LSI_{max}) greater than 1.0 and an LSI_{max} value exceeding 0.25, indicating their relevance as predictors. The size of factors' ranges (maximal value differences per factor) also serves as ranking indicators for the AHP, the second method employed in this study.

In the AHP method, factor weights are determined through pairwise comparisons, resulting in a comparison matrix. The matrix-based weight of the factors and the matrix's consistency ratio (CR) are calculated using the AHP Excel template and online form [63]. The CR is calculated to ensure the matrix's reliability, with a prescribed threshold of less than 0.1 for acceptance [82]. Thus, the CR is 0.035, signifying acceptable consistency.

The factor class ranking (R) is based on the LSI values range and expert rankings. It is defined from 1 (insignificant influence) to 5 (highest influence for that factor). Thus, it is found that the highest number of recorded landslides (95) is present in the slope class of 10–30°, and that class is ranked at the value 5. The same procedure is taken for all other factors, and then factor weights are multiplied by their class rankings. The AHP map is produced by summing the values for all seven factors, i.e., their corresponding classes [63], and the resulting values range from 0.7 (low landslides susceptibility) to 5.0 (high landslides susceptibility).

A hybrid approach is employed to leverage each map's advantages and address potential disadvantages by overlaying both raster grids. The mean sum of LSI and AHP values for each cell is calculated and classified according to natural breaks, resulting in a more refined final map with improved classification accuracy.

Model validation is a critical phase in the LSA methodology. The landslide inventory with 500 recorded landslides and the LSI + AHP model were compared in this process. The findings of this comparison are outlined in Table 7.

Therefore, among the 500 landslides documented, 131 (or 26.2%) are situated within the highest LS zone.

Table 6: AHP comparison matrix for the selected factors

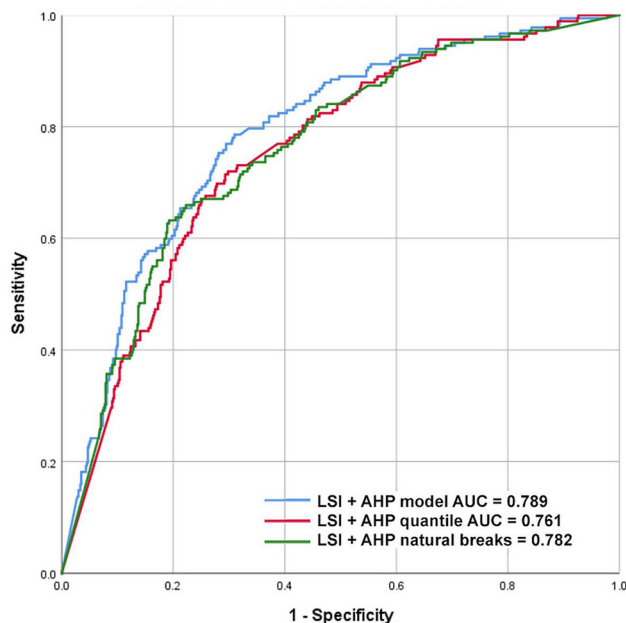
Factor	Slope	Lithology	Land cover	Road dist.	Curvature	Stream dist.	Weight
Slope	1	2	3	4	5	5	0.349
Lithology	0.50	1	2	3	5	5	0.248
Land cover	0.33	1	1	2	3	3	0.152
Road dist.	0.25	0.33	0.50	1	2	3	0.103
Curvature	0.20	0.20	0.33	0.50	1	1	0.058
Stream dist.	0.20	0.20	0.33	0.33	1	1	0.049

Table 7: Recorded landslides by LSI classes and percentages

Class	Registered landslides	In %
1	42	8.4
2	74	14.8
3	128	25.6
4	125	25.0
5	131	26.2
Total	500	100.0

Combined with the high LS zone, this encompasses 51.2% of all observed landslides, indicating a strong accuracy. To comprehensively evaluate the model's performance in the study area, additional validation analysis was conducted using the receiver operating characteristics (ROC) curve and area under the curve (AUC) value (Figure 6). The AUC value serves as a measure of the probabilistic model's reliability in predicting event occurrences. Values between 0.5 and 1 signify a good fit, whereas those below 0.5 indicate randomness. To ensure proper validation, it is recommended to have 2–3 times more false-positive landslides than true ones in the validation dataset [74,82]. In this study, 600 false-positive landslides were randomly selected and thoroughly inspected. The ROC curve and AUC value were computed using SPSS statistical software, resulting in an AUC value of 0.79, signifying a high level of accuracy for the employed model.

Regionally, high and very high landslide susceptibility areas in North Macedonia (29.3%) are predominantly

**Figure 6:** ROC curve and AUC of the combined LSA model.**Table 8:** Landslide susceptibility areas in North Macedonia according to the natural breaks classification

Susceptibility	Class	km ²	%
Very low	1	5512.5	21.4
Low	2	5279.9	20.5
Moderate	3	6953.9	27.0
High	4	3293.2	12.8
Very high	5	4243.3	16.5
Lakes	—	430.3	1.7
Total		25713.0	100.0

located in hilly terrains, mountain foothills, steep valley sides, gorges, and basin slopes covered by Neogene lacustrine sediments (especially in the central, east, and north-east part of the country). Conversely, larger plains and terrains composed of solid rocks, especially in the western part of the country, exhibit lower landslide susceptibility (Table 8; Figure 7). However, field studies reveal that even in these areas, smaller landslides cannot be entirely ruled out, particularly near channels, roads, constructions, and sites with substantial anthropogenic activities.

3.1.2 Multi-hazard modeling

In line with the study's goal, a multi-hazard map was crafted by merging maps depicting erosion and landslide susceptibility. Using SAGA GIS software, regions displaying very high erosion potential were superimposed onto those very highly prone to landslides (Figure 8). This process facilitated the identification of areas facing significant vulnerabilities from both hazards, leading to the delineating of multi-hazard zones. The analysis indicates that parts of North Macedonia are exposed to coexisting threats, specifically landslides and excessive erosion. The multi-hazard zone (3.8%) is typically found in hilly-mountainous regions with steep slopes, non-resistant rocks, and high rainfall intensity. Human activities like deforestation and improper land use exacerbate these vulnerabilities. In Table 9, a zone, calculated as the “total at risk” in the study, covers approximately 22.3% of the country area.

4 Discussion

In North Macedonia, extensive areas experience accelerated erosion due to centuries of intensive human activity in environments conducive to settlement. These regions primarily include steep, south-facing slopes of depressions

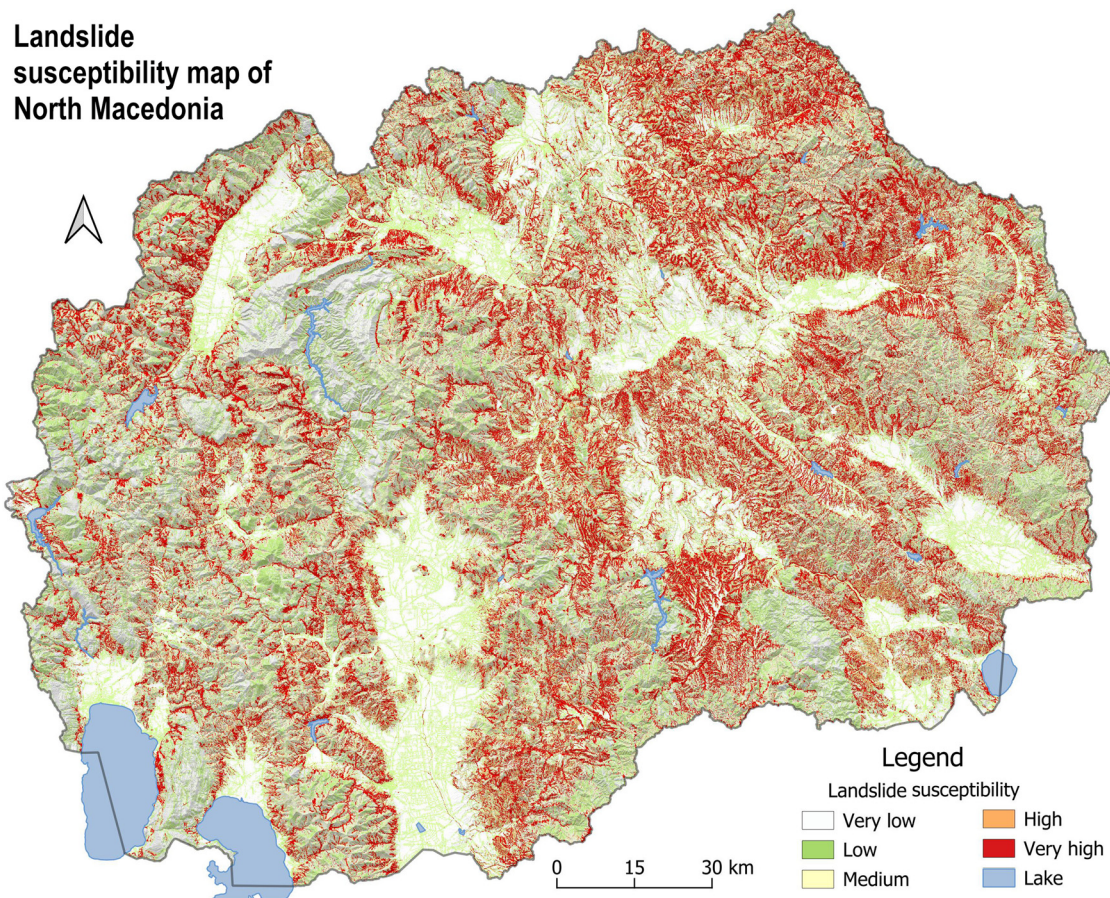


Figure 7: Landslide susceptibility map of North Macedonia based on the mean sum of LSI and AHP values.

and valleys, typically below 1,000 m in elevation, which were favorable for early settlements. The accelerated erosion has transformed the original landscape into rills, gullies, badlands, and earth pyramids. Some landscapes have been severely devastated by soil erosion, notably the Bregalnica catchment, the Crna catchment, and the Pčinja catchment. Conversely, the lower regions of these catchments and valleys experience substantial deposition of eroded material, significantly influencing fluvial processes. The lower sections of rivers such as Vardar, Pčinja, Bregalnica, and Crna are covered by extensive alluvial plains with fresh deposits, where lateral erosion, meandering, and channel accretion prevail. Due to excessive deposition, many downstream riverbeds have been uplifted by more than 10–15 m, resulting in the abandonment of large tracts of agricultural land and significant socioeconomic impacts on rural environments.

According to the results obtained from the EPM, the average value of the erosion coefficient Z for North Macedonia is 0.36, or low-to-moderate. Nevertheless, there is a significant presence of terrains with moderate, high, and very high erosion risk (values greater than 0.4), comprising 8981.3 km² or 35% of the total area.

The average annual sediment production is 516.4 m³/km² or 0.56 mm/year. As much as 13.3% of the total area is under high and very high erosion rates, exceeding 2,000 m³/km²/year (a soil layer of 2 mm per year). Excessive water erosion in these areas causes the creation of eroded landscapes, the loss of fertile areas, and the filling of riverbeds with large amounts of sedimentary material.

According to the available data for the countries in the region, the Republic of Serbia has an average erosion coefficient of 0.3 and a mean erosion rate of about 487.8 m³/km²/year [83]. Slovenia, a country of similar area (20,273 km²), has a specific erosion rate of about 280 m³/km²/year [84], which is nearly half the average specific erosion rate for the territory of North Macedonia (516.4 m³/km²/year). The mean erosion rate on the Republic of Srpska's territory (as a part of BiH) was 239.91 m³/km²/year [53]. On the other side, the mean erosion rate in Greece is much higher – approximately 27.5 tons/ha/year, equivalent to 1,018 m³/km²/year [85].

Aside from the proven accuracy shown in our study, several drawbacks and uncertainties associated with the

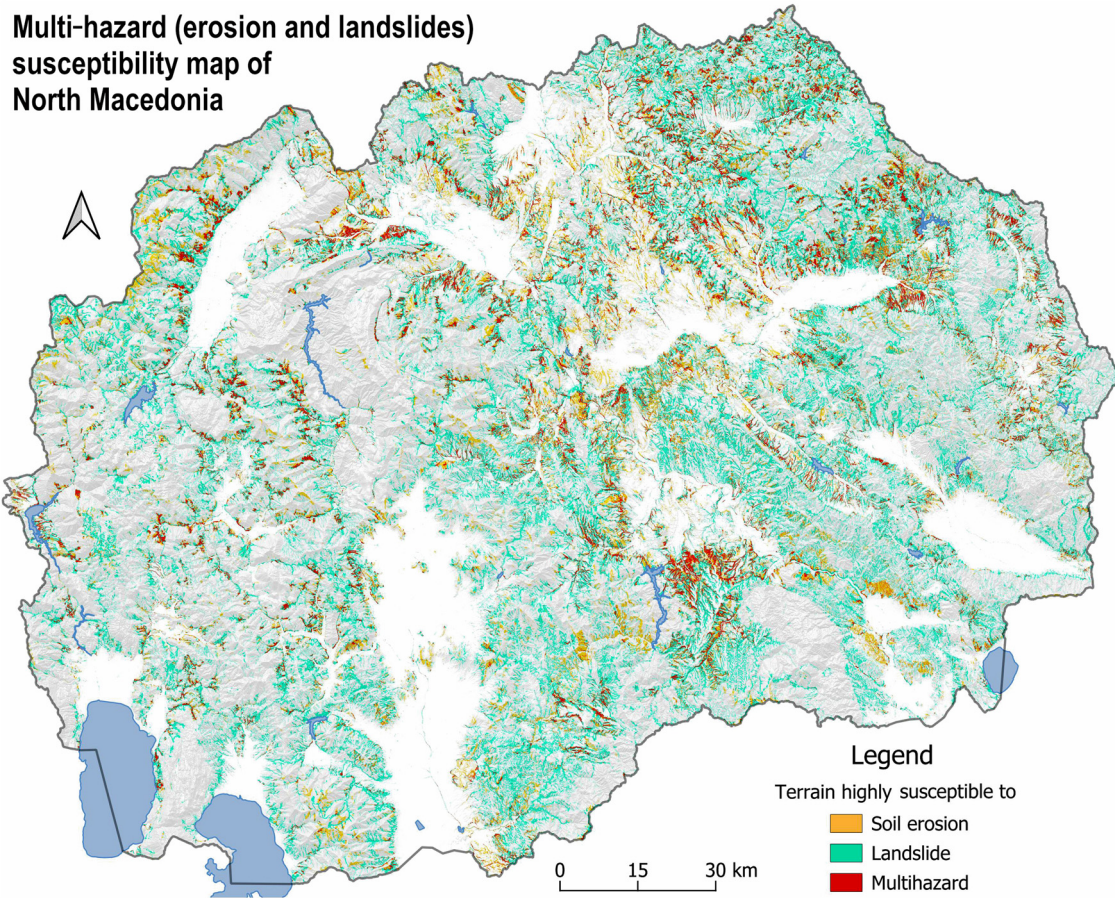


Figure 8: Multi-hazard map of the extended area of North Macedonia.

Table 9: Areas highly susceptible to erosion, landslides, and multi-hazards in North Macedonia (% of total area)

High susceptibility to	km ²	%
Erosion	1491.4	5.8
Landslides	3222.5	12.7
Multi-hazards	971.3	3.8
Total at risk	5685.2	22.3

GIS-based approach of EPM need to be considered in further applications and developments:

- The coefficient of rock and soil erodibility “Y” poses challenges as values are relative and determined by the author of the original model based on estimations. Incorporating and combining these two types of erodibility (rock and soil) into a single value is complex, especially without a high-detail soil properties map for North Macedonia.
- The coefficient “Xa,” related to land use type and closely tied to (CLC) data, presents challenges due to the outdated

CLC2018 model. Changes in land cover, such as forest fires in 2021, 2022, and 2024, are not represented yet, emphasizing the need for updates with the latest satellite imagery.

- In certain cases, using the BSI from satellite imagery as a basis for the coefficient of visible erosion processes φ may not be optimal. Combining spectral bands (red, near infrared – NIR) may provide more accurate values.

One of the primary objectives of this work was to evaluate landslide susceptibility at a regional scale, specifically in North Macedonia. LSA is crucial in anticipating and mitigating potential landslide occurrences or minimizing their impact. At the regional level, statistical methods are widely considered the most suitable for landslide mapping due to their objectivity, reproducibility, and ease of updating [86]. A bivariate statistical analysis conducted in a GIS environment examined the relationships between landslide events and geo-environmental factors, presenting the findings on a susceptibility map. The approach offers two main advantages: it utilizes clear and logical criteria for analysis

and is based on empirical data related to actual landslide events. However, without a comprehensive landslide inventory, statistical approaches can be complemented by semi-quantitative methods like the AHP, which introduces subjectivity into the analysis [63,86].

This study considered six preconditions for landslide occurrence: slope, lithology, land cover, plan curvature, distance from streams, and road distance. These factors were converted into raster (grid) format and standardized to a cell size of 15 m. The frequency ratio of landslide events in each factor class was then calculated as LSI values. These values formed the basis for the relative rankings of factor classes used in the AHP weighting matrix. The final LS model is derived as a mean sum of LSI and AHP values. Five LSZ were classified using natural breaks. Despite a limited landslide inventory, combining the LSI and AHP approach achieves a 79% AUC value, showing accurate results considering the scale of analysis. The results indicate that a significant portion of the country (29.3%) is situated within high and very high landslide susceptibility zones, corroborated by the landslide dataset.

The LSI + AHP approach used in our study has several limitations. As the modeling is based on national-scale datasets, the results are unsuitable for a reliable site-oriented spatial analysis, for which a much more detailed landslide inventory and precondition factors in better resolution are needed. Furthermore, the resulting LS map presents only the predicted spatial distribution of landslides and not the temporal probability of landslide occurrence (for which the exact data about the precipitation patterns and highest intensities must be considered). To improve LSA, a significant improvement of the landslide data inventory is needed, as well as better spatial resolution of the precondition data layers, the inclusion of additional precondition factors (e.g., topographic wetness index, stream power index, normal difference vegetation index, geological structural elements, precipitation intensities, and the introduction of alternative model validation approaches.

By superimposing high erosion and landslide susceptibility zones, a multi-hazard area is identified, covering 3.8% of the national territory. This area is highly susceptible to both soil erosion and landslides and frequently threatens productive land, settlements, infrastructure and even human lives. These sites need to be among the state priorities for protection and conservation. However, other natural and geohazards (like flash floods, ground subsidence, etc.) need to be included in multi-hazard zonation and maps utilizing the recent technologies. In that regard, new methods increasingly rely on machine learning, probabilistic modeling, and data-driven approaches to handle the complexity of natural and

geohazard interactions. Machine learning's ability to process large datasets, detect patterns, and predict hazard events is central to these advancements. Hybrid models that combine machine learning with physical models are becoming more common in leveraging the strengths of both methods. Moreover, real-time monitoring, uncertainty estimation, and the focus on cascading hazard interactions are areas of active research [87,88].

Addressing landslides and excessive erosion is crucial for managing and mitigating geohazards in North Macedonia. Combined with field research, these results are vital for preserving geodiversity values. The findings contribute to understanding erosion vulnerability in Southeast Europe, highlighting specific challenges at the country level.

5 Conclusion

The ultimate goal of creating a reliable and accurate multi-hazard map covering the entire country is to identify vulnerable areas and guide preventive actions and activities to reduce hazard vulnerability. If implemented effectively, such maps are instrumental in minimizing or avoiding future risks and damages [33,89]. This significance becomes even more pronounced when considering climate change forecasts and their potential impact on increased landslide frequency and soil erosion yield. However, in North Macedonia, national funds are predominantly allocated for damage recovery, with a limited focus on prevention and developing high-quality susceptibility models and maps.

One of the principal products of multi-hazard vulnerability studies is maps [90]. Examining areas highly prone to multi-hazards is essential for implementing preventive measures and effective environmental management by local, provincial, and state services [89–91]. A key goal of multi-hazard mapping is to delineate hazardous zones, aiding in reducing vulnerabilities and preventing future damage [92–98]. This is particularly crucial considering the impact of climate change, associated with increased landslide activity and excessive erosion [99]. The approach outlined in this study can potentially create reliable multi-hazard maps nationally, offering valuable insights for regional planning and decision-making processes [100–102]. Using such maps, stakeholders can make informed choices and take measures to minimize vulnerabilities and enhance resilience to environmental challenges. Identification and management of these zones involve comprehensive vulnerability assessments and implementation of mitigation measures such as slope stabilization and reforestation to minimize their impact on communities and infrastructure.

With its distinct physical features, geographical position, and rich geodiversity, North Macedonia provides an ideal context for a comprehensive regional geohazard analysis [34,103]. GIS facilitate the use of relevant data to assess excessive and water erosion, landslide susceptibility, and multi-hazard-prone areas. GIS capabilities allow for a holistic understanding of the interaction between geohazards and the landscape. Nevertheless, the results presented in this article represent the first multi-hazard assessment and the initial version of an integral map of multi-hazard distribution in North Macedonia for land use planning, which is important nationally and regionally. For any specific conclusion, establishing a cadaster of geohazard-endangered areas in the entire country area as a valuable future goal, aiding sustainable spatial and urban planning will be needed.

Acknowledgements: The authors are grateful to the reviewers whose comments and suggestions greatly improved the manuscript.

Author contributions: Conceptualization: I.M. and B.A.; methodology: I.M.; investigation: I.M., S.D., and T.L.; data curation: I.M. and B.A.; writing – original draft preparation: I.M. and B.A.; writing – review and editing: I.M. and B.A.; and formal analysis: S.D., T.L., and A.V.

Conflict of interest: Authors state no conflict of interest.

References

- [1] Lukić T, Marić P, Hrnjak I, Gavrilov MB, Mladjan D, Zorn M, et al. Forest fire analysis and classification based on a Serbian case study. *Acta Geogr Slovenica*. 2017;57(1):51–63. doi: 10.3986/ags.918.
- [2] Aleksova B, Milevski I, Dragičević S, Lukić T. GIS-based integrated multi-hazard vulnerability assessment in Makedonska Kamenica municipality, North Macedonia. *Atmosphere*. 2024;15(7):774. doi: 10.3390/atmos15070774.
- [3] Bathrellos GD, Skilodimou HD, Chousianitis K, Youssef AM, Pradhan B. Suitability estimation for urban development using multi-hazard assessment map. *Sci Total Environ*. 2017;575:119–34. doi: 10.1016/j.scitotenv.2016.10.025.
- [4] Skilodimou HD, Bathrellos GD, Chousianitis K, Youssef AM, Pradhan B. Multi-hazard assessment modeling via multi-criteria analysis and GIS: A case study. *Environ Earth Sci*. 2019;78:47. doi: 10.1007/s12665-018-8003-4.
- [5] Sevieri G, Galasso C, D'Ayala D, De Jesus R, Oreta A, Grieco MEDA, et al. A multi-hazard risk prioritization framework for cultural heritage assets. *Nat Hazards Earth Syst Sci*. 2020;20:1391–414. doi: 10.5194/nhess-20-1391-2020.
- [6] Pourghasemi RH, Kariminejad N, Amiri M, Edalat M, Zarafshar M, Blaschke T, et al. Assessing and mapping multi-hazard risk susceptibility using machine learning techniques. *Sci Rep*. 2020;10:3203. doi: 10.1038/s41598-020-60191-3.
- [7] Muwahhid A, Alwi M, Sari SP, Tilova UDN, Pratama ID. Mapping of multiple hazards in the Cilogkrang Sub-Watershed, Majalengka, Indonesia. *IOP Conf Series: Earth Environ Sci*. 2024;1313:012028. doi: 10.1088/1755-1315/1313/1/012028.
- [8] Lombardo L, Tanyas H, Nicu CI. Spatial modeling of multi-hazard threat to cultural heritage sites. *Eng Geol*. 2020;277:105776. doi: 10.1016/j.enggeo.2020.105776.
- [9] Javidan N, Kaviani A, Pourghasemi RH, Conoscenti C, Jafarian Z, Rodrigo-Comino J. Evaluation of the multi-hazard map produced using MaxEnt machine learning technique. *Sci Rep*. 2021;11:6496. doi: 10.1038/s41598-021-85862-7.
- [10] Milevski I. Natural hazards in the Republic of Macedonia with special emphasis on flood and earthquake in Skopje in 2016. *Geogr Rev*. 2017;50:5–22.
- [11] Milevski I, Dragicevic S, Radevski I. GIS and Remote Sensing based natural hazard modeling of Kriva Reka catchment, Republic of Macedonia. *Z Geomorphol*. 2017;58(Suppl. S3):213–28. doi: 10.1127/zfg_suppl/2016/0364.
- [12] Milevski I, Dragičević S, Zorn M. Statistical and expert-based landslide susceptibility modeling on a national scale applied to North Macedonia. *Open Geosci*. 2019;11:750–64. doi: 10.1515/geo-2019-0059.
- [13] Milevski I, Dragicevic S, Georgievska A. GIS and RS-based modeling of potential natural hazard areas in Pehchevo municipality, Republic of Macedonia. *J Geographical Inst "Jovan Cvijić" SASA*. 2013;63(3):95–107. doi: 10.2298/IJGI13030731.
- [14] Milevski I. An approach of GIS-based assessment of soil erosion rate on country level in the case of Macedonia. In *Proceedings of the Conference Geobalcanica*. Skopje, North Macedonia, 5–7 June 2015, Vol. 1. doi: 10.18509/GBP.2015.13.
- [15] Aleksova B, Lukić T, Milevski I, Spalević V, Marković SB. Modeling water erosion and mass movements (wet) by using GIS-based multi-hazard susceptibility assessment approaches: A case study – Kratovska Reka catchment (North Macedonia). *Atmosphere*. 2023;14(7):1139. doi: 10.3390/atmos14071139.
- [16] Aleksova B, Lukić T, Milevski I, Puhar D, Marković SB. Preliminary assessment of geohazards' impacts on geodiversity in the Kratovska Reka Catchment (North Macedonia). *Geosciences*. 2024;14:62. doi: 10.3390/geosciences14030062.
- [17] Dragicević S, Filipović D, Kostadinov S, Ristić R, Novković I, Zivković N, et al. Natural hazard assessment for land-use planning in Serbia. *Int J Environ Res*. 2011;5(2):371–80.
- [18] Blinkov I, Kostadinov S. Applicability of various erosion risk assessment methods for engineering purposes. In *BALWOIS 2010 Conference - Ohrid*. Republic of Macedonia: 25–29 May 2010.
- [19] Eckelmann W, Baritz R, Bialousz S, Bielek P, Carré F, Houšková B et al. Common criteria for risk area identification according to soil threats. *EUR 22185 EN*. Luxembourg: Office for Official Publications of the European Communities; 2006.
- [20] Alewell C, Borrelli P, Meusburger K, Panagos P. Using the USLE: Chances, challenges and limitations of soil erosion modelling. *Int Soil Water Conserv Res*. 2019;7(3):203–25. doi: 10.1016/j.iswcr.2019.05.004.
- [21] Kirkby M, Irvine BJ, Jones RJA, Govers G. The PESERA coarse scale erosion model for Europe. I. Model rationale and

- implementation. *Eur J Soil Sci.* 2008;59(6):1293–306. doi: 10.1111/j.1365-2389.2008.01072.x.
- [22] Goodrich D, Burns IS, Unkrich CL, Semmens DJ, Guertin D, Hernandez M, et al. KINEROS2/AGWA: Model use, calibration, and validation. *Trans ASABE.* 2012;55(4):1561–74. doi: 10.13031/2013.42264.
- [23] Hagen LJ. Evaluation of the wind erosion prediction system (WEPS) erosion submodel on cropland fields. *Environ Model & Softw.* 2004;19(2):171–6. doi: 10.1016/S1364-8152(03)00119-1.
- [24] Laflen JM, Lane LJ, Foster GR. WEPP: A new generation of erosion prediction technology. *J Soil Water Conserv.* 1991;46(1):34–8.
- [25] Guo T, Srivastava A, Flanagan DC. Improving and calibrating channel erosion simulation in the Water Erosion Prediction Project (WEPP) model. *J Environ Manag.* 2021;291(1):112616. doi: 10.1016/j.jenvman.2021.112616.
- [26] Gavrilović S. Engineering of Torrents and Erosion. *Journal of Construction (Special Issue).* Belgrade, Yugoslavia: 1972. (in Serbian).
- [27] Milevski I. Modeling soil erosion intensity with software tools, in the example of Kumanovo Basin. *Proceedings of II Congress of Macedonian Geographic Society.* Ohrid: 2001. p. 49–57. (in Macedonian).
- [28] Globevnić L, Holjević D, Petkovšek G, Rubinić J. Applicability of the Gavrilović method in erosion calculation using spatial data manipulation techniques. In *Erosion Prediction in Ungauged Basins: Integrating Methods and Techniques.* Wallingford, UK: IAHS Publication; 2003. p. 279.
- [29] Jovanovski M, Gjorgjevski S, Josifovski J, Dolenec K. A landslide in town Veles, from a natural hazard to prevention. *Latest Natural Disasters - New Challenges for Engineering Geology, Geotechnics and Civil Protection.* Sofia; 2005. p. 62–6.
- [30] Reichenbach P, Rossi M, Malamud B, Mihir M, Guzzetti F. A review of statistically-based landslide susceptibility models. *Earth-Sci Rev.* 2018;180:60–91. doi: 10.1016/j.earscirev.2018.03.001.
- [31] Pourghasemi HR, Teimoori Yansari Z, Panagos P, Pradhan B. Analysis and evaluation of landslide susceptibility: a review on articles published during 2005–2016 (periods of 2005–2012 and 2013–2016). *Arab J Geosci.* 2018;11:193. doi: 10.1007/s12517-018-3531-5.
- [32] Chalkias C, Polykretis C, Ferentinou M, Karymbalis E. Integrating expert knowledge with statistical analysis for landslide susceptibility assessment at regional scale. *Geosciences.* 2016;6(14):1–15. doi: 10.3390/geosciences6010014.
- [33] Proske H, Bauer C. Indicative hazard maps for landslides in Styria, Austria. *Acta Geobalkanica.* 2016;2(2):93–101. doi: 10.18509/AGB.2016.10.
- [34] Milevski I. General geomorphological characteristics of the Republic of Macedonia. *Geographical Rev.* 2015;48:5–25.
- [35] Arsovski M. Tectonics of Macedonia. *Faculty of geology and mining.* Štip; 1997. p. 306. (in Macedonian).
- [36] Djordjević M, Trendafilov A, Jelić D, Georgievski S, Popovski A. Erosion map of the Republic of Macedonia - textual part. *Skopje: Water Development Institute;* 1993. p. 89. (in Macedonian).
- [37] Jovanovski M, Milevski I, Papić JB, Peševski I, Markoski B. Landslides in the Republic of Macedonia triggered by extreme events in 2010. In: Loczy D, editor. *In Geomorphological impacts of extreme weather: case studies From Central and Eastern Europe.* Dordrecht, Netherlands: Springer; 2013. p. 265–280. doi: 10.1007/978-94-007-6301-2_17.
- [38] Crozier MJ, Glade T. Landslide hazard, and risk: issues, concepts and approach. In *Landslide Hazard and Risk.* Wiley; 2012. p. 1–39. doi: 10.1002/9780470012659.ch1.
- [39] Gocić M, Dragičević S, Radivojević R, Martić Bursać N, Stričević L, Đorđević M. Changes in soil erosion intensity caused by land use and demographic changes in the Jablanica River Basin, Serbia. *Agriculture.* 2020;10:345. doi: 10.3390/agriculture10080345.
- [40] De Vente J, Poesen J. Predicting soil erosion and sediment yield at the basin scale: scale issue and semi-quantitative models. *Earth-Sci Rev.* 2005;71:95–125. doi: 10.1016/j.earscirev.2005.02.002.
- [41] De Vente J, Poesen J, Bazzoffi B, Van Rompaey A, Verstraeten G. Predicting catchment sediment yield in Mediterranean environments: The importance of sediment sources and connectivity in Italian drainage basins. *Earth Surf Process Landf.* 2006;31:1017–34. doi: 10.1002/esp.1305.
- [42] Efthimiou N, Lykoudi E, Panagoulia D, Karavitis C. Assessment of soil susceptibility to erosion using the EPM and RUSLE models: The case of Venetikos river catchment. *Glob NEST J.* 2016;18:164–79.
- [43] Dragičević N, Karleuša B, Ožanić N. A review of the Gavrilović method (erosion potential method) application. *Građevinar J Croat Assoc Civ Eng.* 2016;68:715–25. doi: 10.14256/JCE.1602.2016.
- [44] Bezak N, Borrelli P, Mikoš M, Auflić MJ, Panagos P. Towards multi-model soil erosion modelling: an evaluation of the erosion potential method (EPM) for global soil erosion assessments. *CATENA.* 2024;234:107596. doi: 10.1016/j.catena.2023.107596.
- [45] Petras J, Holjević D, Kunstek D. Implementation of GIS-technology in Gavrilović's method for estimation soil erosion production and sediment transport. In *Proceedings of the International Conference Erosion and Torrent Control as a Factor in Sustainable River Basin Management.* Belgrade, Serbia: 25–28 September 2007.
- [46] Federal Geological Survey of SFRY (1963–1985), Interpreter of the Basic Geological Map of Socialist Federal Republic of Yugoslavia 1:100,000 (Sheet 25 for SR Macedonia), Professional Fund of the Federal Geological Survey of SFRY, Belgrade, Yugoslavia, (In Macedonian).
- [47] FAO. Soil Map of the Republic of Macedonia, 1:50,000; FAO: Rome, Italy; Skopje, North Macedonia: Agricultural Institute-UKIM; 2015. (In Macedonian).
- [48] Corine Land Cover 2018. Copernicus land monitoring service. In *Technical Report;* Luxembourg: Office for Official Publications of the European Communities; 2016.
- [49] Milevski I. Factors, forms, assessment and human impact on excess erosion and deposition in upper Bregalnica watershed (Republic of Macedonia). In: Harnischmacher S, Loczy D, editors. *Human impact on landscape.* Stuttgart: 2011. *Zeitschrift für Geomorphologie, Vol. 55, Supplementary issue 1;* p. 77–94. doi: 10.1127/0372-8854/2011/0055S1-0039.
- [50] Durlević U, Novković I, Lukić T, Valjarević A, Samardžić I, Krstić F, et al. Multihazard susceptibility assessment: A case study – Municipality of Štrpce (Southern Serbia). *Open Geosci.* 2021;13:1414–31. doi: 10.1515/geo-2020-0314.
- [51] Fick SE, Hijmans RJ. Worldclim 2: New 1-km Spatial Resolution Climate Surfaces for Global Land Areas. *Int J Climatol.* 2017;37:4302–15.
- [52] Wan Z, Hook S, Hulley G. MOD11A1 MODIS/Terra Land Surface Temperature/Emissivity Daily L3 Global 1km SIN Grid V006. NASA EOSDIS Land Processes DAAC. Accessed 2024-05-29. doi: 10.5067/MODIS/MOD11A1.006.

- [53] Tosić R, Dragičević S, Lovrić N. Assessment of soil erosion and sediment yield changes using erosion potential model – Case study: Republic of Srpska (BiH). *Carpathian J Earth Environ Sci*. 2012;7:147–54.
- [54] Spalević V, Barović G, Vujčić D, Curović M, Behzadfar M, Djurović N, et al. The Impact of Land Use Changes on Soil Erosion in the River Basin of Miocki Potok, Montenegro. *Water*. 2020;12:2973. doi: 10.3390/w12112973.
- [55] Kostadinov S, Braunović S, Dragičević S, Zlatić M, Dragović N, Rakonjac N. Effects of erosion control works: case study – Grdelica Gorge, the South Morava River (Serbia). *Water*. 2018;10:1094. doi: 10.3390/w10081094.
- [56] Zorn M, Komac B. The importance of measuring erosion processes on the example of Slovenia. *Hrvat Geogr Glas*. 2011;73:19–34.
- [57] Kazimierski LD, Irigoyen M, Re M, Menendez AN, Spalletti P, Brea JD. Impact of climate change on sediment yield from the upper Plata Basin. *Int J River Basin Manag*. 2013;11:411–21. doi: 10.1080/15715124.2013.828066.
- [58] Tavares AS, Spalević V, Avanzi JC, Alves D. Modeling of water erosion by the erosion potential method in a pilot subbasin in southern Minas Gerais. *Semin Ciências Agrárias Londrina*. 2019;40:555–72. doi: 10.5433/1679-0359.2019v40n2p555.
- [59] Ali S, Al-Umary FA, Salar SG, Al-Ansari N, Knutsson S, GIS-Based Soil Erosion Estimation Using EPM Method, Garmiyān Area, Kurdistan Region, Iraq. *J Civ Eng Archit*. 2016;10:291–308. doi: 10.17265/1934-7359/2016.03.006.
- [60] Hazbavi Z, Azizi E, Sharifi Z, Alaei N, Mostafazadeh R, Behzadfar M, et al. Comprehensive estimation of erosion and sediment components using intero model in the Koozeh Topraghi watershed. *Ardabil Province Env Eros Res J*. 2020;10:92–110.
- [61] Behzadfar M, Tazioli A, Vukleic-Shutoska M, Simunic I, Spalevic V. Calculation of sediment yield in the S1-1 watershed, shirindareh watershed. *Iran Agric For*. 2014;60:207–16. doi: 10.17707/AgricultForest.60.3.20.
- [62] Tošić R, Dragičević S, Lovrić N, Milevski I. Multi-hazard assessment using GIS in urban areas: Case study - Banja Luka municipality. *Bosnia Herzeg Bull Serb Geogr Soc*. 2013;93(4):41–50. doi: 10.2298/GSGD1304041T.
- [63] Milevski I, Dragičević S. Landslides susceptibility zonation of the territory of North Macedonia using the analytical hierarchy process approach. *Sect Nat Math Biotech Sci MASA*. 2019;40:115–26. doi: 10.20903/csnmbs.masa.2019.40.1.135.
- [64] Varnes DJ. Slope movement types and processes. In: Schuster RL, Krizek RJ, editors. *Landslides, Analysis and Control; Special Report 176*. Transportation Research Board. Washington, DC: National Academy of Sciences; 1978. p. 11–33.
- [65] Crozier M. *Landslides: Causes, Consequences, and Environment*. London: Croom Helm; 1986. p. 252.
- [66] Donati L, Turrini MC. An objective method to rank the importance of the factors predisposing to landslides with the GIS methodology: Application to an area of the Apennines (Valnerina; Perugia, Italy). *Eng Geol*. 2002;63(3–4):277–89. doi: 10.1016/S0013-7952(01)00087-4.
- [67] Dragičević S, Carević I, Kostadinov S, Novković I, Abolmasov B, Milojković B, et al. Landslide susceptibility zonation in the Kolubara River Basin (western Serbia) – analysis of input data. *Carpathian J. Earth Environ. Sci*. 2012;7(2):37–47.
- [68] Jaafari A, Najafi A, Pourghasemi HR, Rezaei A, Sattarian A. GIS-based frequency ratio and index of entropy models for landslide susceptibility assessment in the Caspian Forest, northern Iran. *Int J Environ Sci Technol*. 2014;11(4):909–26. doi: 10.1007/s13762-013-0464-0.
- [69] Magliulo P, Di Lisio A, Russo F, Zelando A. Geomorphology and landslide susceptibility assessment using GIS and bivariate statistics: A case study in southern Italy. *Nat Hazards*. 2008;47:411–35. doi: 10.1007/s11069-008-9230-x.
- [70] He Y, Beighley RE. GIS-based regional landslide susceptibility mapping: A case study in southern California. *Earth Surf Process Landf*. 2008;33:380–93. doi: 10.1002/esp.1562.
- [71] Tanaka Y. Differences of Landslide Occurrences Behavior Due to Slope Aspects in the Amehata River Basin. *American Geophysical Union, Fall Meeting*; 2005.
- [72] Wu C, Ding M, Wang Q, Qiao J. Correlation between landslides and gradient in the Three Gorges Reservoir area based on GIS and information value model. In 2010 18th International Conference on Geoinformatics; 2010. p. 1–5.
- [73] Bathrellos GD, Kalivas DP, Skilodimou HD. GIS-based landslide susceptibility mapping models applied to natural and Urban Planning in Trikala, Central Greece. *Estudios Geológicos*. 2009;65(1):49–65. doi: 10.3989/egol.08642.036.
- [74] Mărgărint MC, Grozavu A, Patriche CV. Assessing the spatial variability of coefficients of landslide predictors in different regions of Romania using logistic regression. *Nat Hazards Earth Syst Sci*. 2013;13(12):3339–55. doi: 10.5194/nhess-13-3339-2013.
- [75] Süzen ML, Doyuran V. A comparison of the GIS-based landslide susceptibility assessment methods: Multivariate versus bivariate. *Env Geol*. 2004;45(5):665–79. doi: 10.1007/s00254-003-0917-8.
- [76] Jenks GF. *Optimal Data Classification for Choropleth Maps*. Kansas: Dept Geography, Univ Kansas; 1977.
- [77] Stegna L, Csillag F. Statistical determination of class intervals for maps. *Cartogr J*. 1987;24(2):142–6.
- [78] Süzen M, Doyuran V. Data-driven bivariate landslide susceptibility assessment using geographical information systems: A method and application to Asarsuyu catchment, Turkey. *Eng Geol*. 2004;71:303–21. doi: 10.1016/S0013-7952(03)00143-1.
- [79] United Nations Office for Disaster Risk Reduction, Available at: <https://www.undrr.org/> (Accessed on 29 April 2024).
- [80] Dragičević S, Mészáros M, Djurdjic S, Pavić D, Novković I, Tošić R. Vulnerability of national parks to natural hazards in the Serbian Danube region. *Pol J Environ Stud*. 2013;22(4):75–82.
- [81] Minčev I, Blinkov I, Trendafilov A. Sedimentation rates and life-span analyses in the reservoir “Kalimanci”. *Sect Nat Math Biotechnol Sci MASA*. 2019;40(2):181–9. doi: 10.20903/csnmbs.masa2019.40.2.142.
- [82] Chalkias C, Ferentinou M, Polykretis C. GIS-Based Landslide Susceptibility Mapping on the Peloponnese Peninsula, Greece. *Geosciences*. 2014;4(3):176–90. doi: 10.3390/geosciences4030176.
- [83] Veličković N, Todosijević M, Šulić D. Erosion Map Reliability Using a Geographic Information System (GIS) and Erosion Potential Method (EPM): A Comparison of Mapping Methods, BELGRADE Peri-Urban Area, Serbia. *Land*. 2022;11:1096. doi: 10.3390/land11071096.
- [84] Komac B, Zorn M. Soil erosion on agricultural land in Slovenia - Measurements of rill erosion in the Besnica valley. *Acta Geographica Slovenica*. 2005;45(1):53–86. doi: 10.3986/AGS45103.
- [85] Panagos P, Borrelli P, Poesen J, Ballabio C, Lugato E, Meusburger K. The New Assessment of Soil Loss by Water Erosion in Europe. *Env Sci Policy*. 2015;54:438–47. doi: 10.1016/j.envsci.2015.08.012.

- [86] Komac M. A landslide susceptibility model using the analytical hierarchy process method and multivariate statistics in perialpine Slovenia. *Geomorphology*. 2006;74:17–28. doi: 10.1016/j.geomorph.2005.07.005.
- [87] Yang C, Liu LL, Huang F, Huang L, Wang XM, et al. Machine learning-based landslide susceptibility assessment with optimized ratio of landslide to non-landslide samples. *Gondwana Res*. 2023;123:198–216. doi: 10.1016/j.gr.2022.05.012.
- [88] Gill JC, Malamud BD. Anthropogenic processes, natural hazards, and interactions in a multi-hazard framework. *Earth Sci Rev*. 2017;166:246–69.
- [89] Singh B, Goel RK. Landslide hazard zonation. In rock mass classification. 1st edn. Elsevier Science; 1999. p. 184–199.
- [90] Kappes M, Keiler M, Elverfeldt K-V, Glade T. Challenges of dealing with multi-hazard risk: a review. *Nat Hazards*. 2012;64(2):1925–58. doi: 10.1007/s11069-012-0294-2.
- [91] Antofie T-E, Luoni S, Tilloy A, Sibilia A, Salari S, Eklund G, et al. Spatial identification of regions at risk to multi-hazards at the pan-European level: an implemented methodological approach. *Nat Hazards Earth Syst Sci*. 2024. doi: 10.5194/nhess-2023-220.
- [92] Micu M, Sima M, Balteanu D, Micu D, Dragotă C, Chendeş V. A multi-hazard assessment in the Bend Carpathians of Romania. Conference: Mountain Risks: Bringing Science to Society, Florence, Italy; 2010.
- [93] Tempa K, Yuden K. Multi-hazard zoning for national scale population risk mapping: a pilot study in Bhutan Himalaya. *Geoenviron Disasters*. 2023;10(7):1–15. doi: 10.1186/s40677-023-00239-4.
- [94] Ulza A, Idris Y, Asyifa CN, Irvansyah R. Closing the resilience gap: a preliminary study on establishing the national fragility curve catalog for multi-hazard assessment in Indonesia. *E3S Web Conf*. 2023;443:01002. doi: 10.1051/e3sconf/202344701002.
- [95] Carrara A, Cardinali M, Guzzetti F, Reichenbach P. GIS technology in mapping landslide hazard. In *Geographical information systems in assessing natural hazards*. Advances in natural and technological hazards research. Dordrecht: Springer; 1995. p. 135–75. doi: 10.1007/978-94-015-8404-3_8.
- [96] Cascini L. Applicability of landslide susceptibility and hazard zoning at different scales. *Eng Geol*. 2008;102(3–4):164–77. doi: 10.1016/j.enggeo.2008.03.016.
- [97] De Graff JV, Romesburg HC, Ahmad R, McCalpin JP. Producing landslide-susceptibility maps for regional planning in data-scarce regions. *Nat Hazards*. 2012;64:729–49. doi: 10.1007/s11069-012-0267-5.
- [98] Guzzetti F, Reichenbach P, Ardizzone F, Cardinali M, Galli M. Estimating the quality of landslide susceptibility models. *Geomorphology*. 2006;81(1–2):166–84. doi: 10.1016/j.geomorph.2006.04.007.
- [99] Micić Ponjiger T, Lukić T, Wilby RL, Marković SB, Valjarević A, Dragičević S, et al. Evaluation of rainfall erosivity in the western Balkans by mapping and clustering ERA5 reanalysis data. *Atmosphere*. 2023;14:104. doi: 10.3390/atmos14010104.
- [100] Saro L, Woo J, Kwan-Young O, Mounj-Jin L. The spatial prediction of landslide susceptibility applying artificial neural network and logistic regression models: A case study of Inje, Korea. *Open Geosci*. 2016;8:117–32. doi: 10.1515/geo-2016-0010.
- [101] Varnes DJ. Landslide hazard zonation: a review of principles and practice. Paris: United Nations Educational, Scientific and Cultural Organization; 1984.
- [102] Tošić R, Dragičević S, Zorn M, Lovrić N. Landslide susceptibility zonation: A case study of the municipality of Banja Luka (Bosnia and Herzegovina). *Acta Geogr Slovenica*. 2014;54(1):189–202. doi: 10.3986/AGS54307.
- [103] Kolčakovski D, Milevski I. Recent landform evolution in Macedonia. Recent landform evolution. In: Loczy D, Stankoviansky M, Kotarba A, editors. *The Carpatho-Balkan-Dinaric Region*. Dordrecht, Netherlands: Springer; 2012. p. 413–442. doi: 10.1007/978-94-007-2448-8_15.